Magnetization Dynamics and Power Loss Calculation in NO Soft Magnetic Steel Sheets Under Arbitrary Excitation

Martin Petrun[1], Simon Steentjes[2], Kay Hameyer[2], and Drago Dolinar[1]

[1]Institute of Power Engineering, FERI, University of Maribor, Maribor SI-2000, Slovenia
[2]Institute of Electrical Machines, RWTH Aachen University, Aachen D-52062, Germany

This paper deals with the analysis of a 1-D magneto-dynamic model (MDM) of soft magnetic steel sheets (SMSSs) under arbitrary excitation conditions. In the presented analysis, the MDM is coupled with the static hysteresis model proposed by Tellinen. The coupled model of SMSSs is evaluated using measured excitation voltages as well as measured excitation currents directly as the model input variables, where both excitation cases are compared and evaluated versus measurements. The calculated results show a good agreement with the measurements. Based on the presented analysis properties, advantages, and flexibility of the MDM model as well as the limitations of the presented coupled model are pointed out, where guidelines for an improved coupling are also given.

Index Terms— **Dynamic modeling, eddy currents, loss separation, magnetic hysteresis, power loss, skin effect, soft magnetic materials.**

I. Introduction

THE number of magnetic components exposed to complex excitation waveforms is nowadays rapidly increasing mainly due to the fast development and increased use of power electronic devices. Over recent decades, various models have been developed for predicting of electromagnetic variables and power losses inside such magnetic components [1]–[7]. Most of these models are based on the 1-D approximation of the electromagnetic field inside the magnetic material as such models often offer an adequate accuracy along with a good computational performance and can be therefore used as a part of different circuit simulation packages. The additional motivation for using individual models inside such packages is, however, often also the simplicity of implementation and flexibility of the used model.

The first objective of this paper is to analyze the performance of the magneto-dynamic model (MDM) [6], [7] soft magnetic steel sheets (SMSSs) under complex excitation waveforms. The discussed MDM is coupled with the hysteresis model proposed by Tellinen (TLN) [8], which describes the static hysteresis relationship of the observed SMSS. Such a coupled model of SMSSs has shown a very good agreement with the measurements for a sinusoidal excitation, where only symmetric minor hysteresis loops were evaluated [6], [7]. In this paper, the analysis of the discussed coupled model is extended to more complex excitation waveforms, such as a sinusoidal excitation containing higher harmonics and pulsewidth modulated (PWM) excitation waveforms that generate complex magnetization curves with offset minor loops. The second objective is to evaluate the usability and flexibility of the discussed model. Therefore, the model predictions are calculated based on the measured current i_p as well as on the measured voltage u_p in the excitation winding, where the results are evaluated by comparing them to measured values on an Epstein frame. Based on the presented analysis, limitations of the coupled model are pointed out and guidelines for an improved coupling are given as well.

Manuscript received June 13, 2014; revised September 3, 2014; accepted September 11, 2014. Date of current version January 26, 2015. Corresponding author: M. Petrun (e-mail: martin.petrun@um.si).

Color versions of one or more of the figures in this paper are available online at http://ieeexplore.ieee.org.

Digital Object Identifier 10.1109/TMAG.2014.2358273

II. Theoretical Background

A. Magneto-Dynamic Model of a SMSS

The discussed MDM is based on the 1-D approximation of the electromagnetic phenomena inside SMSSs. Such an approximation is valid when modeling long and thin conductive SMSSs with predominately small magnetic domains, e.g., non-oriented (NO) SMSSs [6], [7]. In the discussed MDM, the observed SMSSs are virtually divided into N_s equally thick slices. A similar approach is also applied when modeling electromagnetic diffusion phenomena using magnetic equivalent circuits (MECs) [1]–[4]. Using such an approach, a ladder network is obtained, which represents the MEC model of the virtually sliced SMSS. Solving MEC models, the main challenge represents establishing an efficient coupling scheme between the electric and magnetic domains, where different schemes have been proposed in [2]. Although the basic coupling schemes are generally simple, the presence of unknown eddy currents complicates the obtained model. In contrast to this, the MDM proposed in [6] is expressed in form of a simple matrix differential (1) that is describing the equilibriums of magnetomotive forces (MMFs) in all the slices of the SMSS without the need to calculate the eddy currents inside individual slices

$$\begin{aligned}\boldsymbol{\Theta} &= \mathbf{N}i_\mathrm{p} = \bar{\mathbf{H}}\left(\bar{\boldsymbol{\Phi}}\right) l_\mathrm{m} + \mathbf{L}_\mathrm{m}\frac{d\bar{\boldsymbol{\Phi}}}{dt} = \mathbf{R}_\mathrm{m}\bar{\Phi} + \mathbf{L}_\mathrm{m}\frac{d\bar{\boldsymbol{\Phi}}}{dt} \\ &= \boldsymbol{\Theta}_\mathrm{Rm} + \boldsymbol{\Theta}_\mathrm{Lm}. \end{aligned} \tag{1}$$

In (1), $\boldsymbol{\Theta}$ represents a vector of the MMFs generated by the applied current i_p in the excitation winding, $\bar{\mathbf{H}}(\bar{\boldsymbol{\Phi}})$ is a vector of average magnetic field strengths as non-linear (hysteretic) functions of the average magnetic fluxes in the slices, and l_m is the mean length of the magnetic path. The contributions

of MMFs inside the SMSS can be divided into MMFs $\boldsymbol{\Theta}_{\mathrm{Rm}}$ caused by nonlinear reluctances $\mathbf{R}_{\mathrm{m}}$ due to the static hysteresis and MMFs $\boldsymbol{\Theta}_{\mathrm{Lm}}$ caused by the magnetic inductance $\mathbf{L}_{\mathrm{m}}$ due to eddy currents inside individual slices. The vector of excitation winding turns $\mathbf{N}$ is defined by (2), as all the slices are excited with the current i_{p} in the excitation winding

$$\mathbf{N} = N[1]_{N_{\mathrm{s}}\times 1}. \tag{2}$$

Finally, the matrix of magnetic inductance $\mathbf{L}_{\mathrm{m}}$ is defined by (3) and depends only on the geometric and material properties as well as on the discretization of the observed SMSS, where b is the thickness, a is the width, $A_{\mathrm{Fe}} = a \cdot b$ is the cross section, and σ is the specific electric conductivity of the SMSS. The thickness b_{s} of each virtual slice as well as the dimensions of the matrix of magnetic inductance $\mathbf{L}_{\mathrm{m}}$ depend on the discretization of the SMSS, i.e., the number of slices N_{s}

$$\mathbf{L}_{\mathrm{m}} = c \begin{bmatrix} (N_{\mathrm{s}}-1)+\frac{1}{3} & (N_{\mathrm{s}}-2)+\frac{1}{2} & \cdots & 1+\frac{1}{2} & \frac{1}{2} \\ (N_{\mathrm{s}}-2)+\frac{1}{2} & (N_{\mathrm{s}}-2)+\frac{1}{3} & \cdots & 1+\frac{1}{2} & \frac{1}{2} \\ \vdots & \vdots & \ddots & \vdots & \vdots \\ 1+\frac{1}{2} & 1+\frac{1}{2} & \cdots & 1+\frac{1}{3} & \frac{1}{2} \\ \frac{1}{2} & \frac{1}{2} & \cdots & \frac{1}{2} & \frac{1}{3} \end{bmatrix}_{N_{\mathrm{s}}\times N_{\mathrm{s}}} \tag{3}$$

$$c = \sigma l_{\mathrm{m}} \left(\frac{b}{2N_{\mathrm{s}}}\right)^2 \left(\frac{N_{\mathrm{s}}}{A_{\mathrm{Fe}}}\right) = \frac{\sigma l_{\mathrm{m}} b_{\mathrm{s}}}{2a}, \quad b_{\mathrm{s}} = \frac{b}{2N_{\mathrm{s}}}. \tag{4}$$

The number of slices N_{s} can be adopted according to the excitation dynamics and material properties, which also define the penetration depth of the magnetic field. For lower excitation dynamics, coarser discretization is required (less slices), whereas for the higher excitation dynamics, finer discretization is required. Adequate discretization can be obtained, e.g., following the guidelines presented in [4].

Using adequate discretization, the electromagnetic diffusion phenomena inside the observed SMSS are fully described by (1), where the non-linear properties of the individual slices are taken into account using an adequate hysteresis model. The coupling between the magnetic and electric domains simply represents the current i_{p} that flows through the excitation winding. Using the presented MDM, the diffusion phenomena can be calculated based on current i_{p}, which can be an arbitrary function of time. In addition, the discussed model can also be applied to voltage driven problems, which is very important, e.g., when applying the MDM to circuit models. For this purpose, the presented MDM is simply extended by a model of excitation winding (5), where u_{p} and u_{i} represent the applied and induced voltage in the winding and R_{p} and $L_{\sigma\mathrm{p}}$ represent the resistance and leakage inductance of the excitation winding, respectively

$$u_{\mathrm{p}} = i_{\mathrm{p}}R_{\mathrm{p}} + \frac{di_{\mathrm{p}}}{dt}L_{\sigma\mathrm{p}} + u_{\mathrm{i}} = i_{\mathrm{p}}R_{\mathrm{p}} + \frac{di_{\mathrm{p}}}{dt}L_{\sigma\mathrm{p}} + \mathbf{N}^{\mathrm{T}}\frac{d\bar{\boldsymbol{\Phi}}}{dt}. \tag{5}$$

B. Static Hysteresis Description

The matrix differential equation (1) is highly non-linear due to the nature of SMSSs. The non-linear properties of SMSSs can be taken into account coupling the MDM with an adequate hysteresis model. The choice of the applied hysteresis model depends on the application and purpose of the MDM, where in general various hysteresis models can be applied. In this paper, a simple scalar TLN hysteresis model is used [8]. This model is applied due to its uncomplicated implementation and identification as well as good computational performance. The TLN model is based on the major (limit) hysteresis loop, where $B_1^+ = f(H)$ and $B_1^- = f(H)$ represent non-linear functions or table data sets that adequately describe the ascending and descending branches of the limit hysteresis loop as a function of magnetic field strength H. The corresponding slopes of discussed functions $\mu_1^+ = f(H)$ and $\mu_1^- = f(H)$ describe the permeability of the ascending and descending branches as a function of magnetic field strength H. Based on the identified material relations, the TLN model is expressed in the form of two differential equations (6) and (7), which are describing the ascending and descending magnetization curves in individual slices $s \in [1, N_{\mathrm{s}}]$ inside the SMSS

$$\frac{d\bar{H}_{\mathrm{s}}\left(\bar{B}_{\mathrm{s}}\right)}{dt} = \frac{d\bar{B}_{\mathrm{s}}}{dt}\left[\mu_0 + \left(\mu_1^+ - \mu_0\right)\frac{B_1^- - \bar{B}_{\mathrm{s}}}{B_1^- - B_1^+}\right]^{-1}; \quad \frac{d\bar{B}_{\mathrm{s}}}{dt} > 0 \tag{6}$$

$$\frac{d\bar{H}_{\mathrm{s}}\left(\bar{B}_{\mathrm{s}}\right)}{dt} = \frac{d\bar{B}_{\mathrm{s}}}{dt}\left[\mu_0 + \left(\mu_1^- - \mu_0\right)\frac{\bar{B}_{\mathrm{s}} - B_1^+}{B_1^- - B_1^+}\right]^{-1}; \quad \frac{d\bar{B}_{\mathrm{s}}}{dt} < 0. \tag{7}$$

Considering all the slices of the SMSS, the TLN model is coupled with (1) using

$$\frac{d}{dt}\bar{\boldsymbol{\Phi}} = \left(\frac{A_{\mathrm{Fe}}}{N_{\mathrm{s}}}\right)\frac{d}{dt}\bar{\mathbf{B}}. \tag{8}$$

One of the main limitations of the TLN model is that this model does not directly take the previous history of the magnetization process into account. This limitation is further evaluated in Section III, where measured and calculated complex magnetization waveforms are compared.

C. Power Loss Calculation

In engineering, the power loss calculation is indispensable. The presented MDM enables to predict not only arbitrary transient states, but also the power loss distributions inside SMSSs, where the power loss distributions due to static hysteresis effects and eddy currents are considered separately. Similar to the solution of the diffusion phenomena with (1), there is no need to calculate the eddy currents inside the SMSSs as both mentioned power components are calculated directly on the varying densities of magnetic fluxes B_{s} inside individual slices [7]. Therefore, the instantaneous power components can simply be calculated either in parallel with (1) or during the post-processing.

The instantaneous conduction power loss $p_{\mathrm{es}}(t)$ due to eddy currents within each slice is calculated by (9). Furthermore, instantaneous powers $p_{\mathrm{hs}}(t)$ due to the static hysteresis effects

inside slices are calculated by (10), where the calculation of $p_{\mathrm{hs}}(t)$ is independent of the applied hysteresis model

$$p_{\mathrm{es}} = 2\sigma a l_{\mathrm{m}} b_{\mathrm{s}}^3 \left[\left(\sum_{i=1}^{\mathrm{s}-1} \frac{d\bar{B}_i}{dt} \right)^2 + \left(\sum_{i=1}^{\mathrm{s}-1} \frac{d\bar{B}_i}{dt} \right) \frac{d\bar{B}_{\mathrm{s}}}{dt} + \frac{1}{3} \left(\frac{d\bar{B}_{\mathrm{s}}}{dt} \right)^2 \right] \quad (9)$$

$$p_{\mathrm{hs}} = a b_{\mathrm{s}} l_{\mathrm{m}} \bar{H}_{\mathrm{s}} \frac{d\bar{B}_{\mathrm{s}}}{dt}. \quad (10)$$

Note also that $p_{\mathrm{hs}}(t)$ in contrast with $p_{\mathrm{es}}(t)$ does not represent the (static) hysteresis losses, but rather powers that can also be negative due to the nature of the hysteresis magnetization processes. The hysteresis losses are therefore calculated for characteristic time periods Δt. Using (9) and (10), energies W_{es} and W_{hs} and average powers P_{es} and P_{hs} within an arbitrary observed time period $\Delta t = (t_2 - t_1)$ inside individual slice s are calculated by

$$P_{\mathrm{es}} = \frac{W_{\mathrm{es}}}{\Delta t} = \frac{1}{\Delta t} \int_{t_1}^{t_2} p_{\mathrm{es}}(t) dt,\ P_{\mathrm{hs}} = \frac{W_{\mathrm{hs}}}{\Delta t} = \frac{1}{\Delta t} \int_{t_1}^{t_2} p_{\mathrm{hs}}(t) dt. \quad (11)$$

The total instantaneous powers p_{e} and p_{h}, energies W_{e} and W_{h} and the average power loss components P_{e}, P_{h}, and $P_{\mathrm{loss}} = P_{\mathrm{e}} + P_{\mathrm{h}}$ for the entire SMSS are obtained by summing the components of the individual slices.

III. Result

Experimental evaluation has been carried out for samples of grade M400-50A NO 3.2% Fe–Si SMSS of thickness 0.5 mm using the Epstein frame within a computer-aided setup in accordance with the international standard IEC 60404-2. The geometric and material data of the evaluated sample is presented in [6]. The static TLN hysteresis model was identified using quasi-static measurements of the hysteresis loop at $B_{\max} = 1.6$ T, where the model functions are given in the form of adequate lookup tables. The presented model was evaluated for both the current [using just (1)] and voltage [considering also (5)] excitation cases, where the measured currents or voltages were used directly as the model input variables. In the voltage excitation case, the used resistance and leakage inductances of the excitation winding were determined as $R_{\mathrm{p}} = 0.5\ \Omega$ and $L_{\sigma \mathrm{p}} = 1$ nH, respectively.

The measured variables used as model inputs for three different complex magnetization excitations along with the calculated results are shown in Fig. 1. In Fig. 1(a) and (b), the measured and calculated excitation winding voltages u_{p} and currents i_{p} for the case of sinusoidal voltage excitation of frequency $f = 200$ Hz with added 5th harmonic with a phase shift of 45° are shown. The measured voltage u_{p} in Fig. 1(a) is used for the calculation of a excitation current i_{p} in Fig. 1(b) and vice versa. This way the MDM model is evaluated for both discussed excitation cases. The discussed model was further evaluated using arbitrary (PWM like) excitation voltages of the fundamental frequency $f = 50$ Hz as shown in Fig. 1(c) and (e), where the corresponding currents

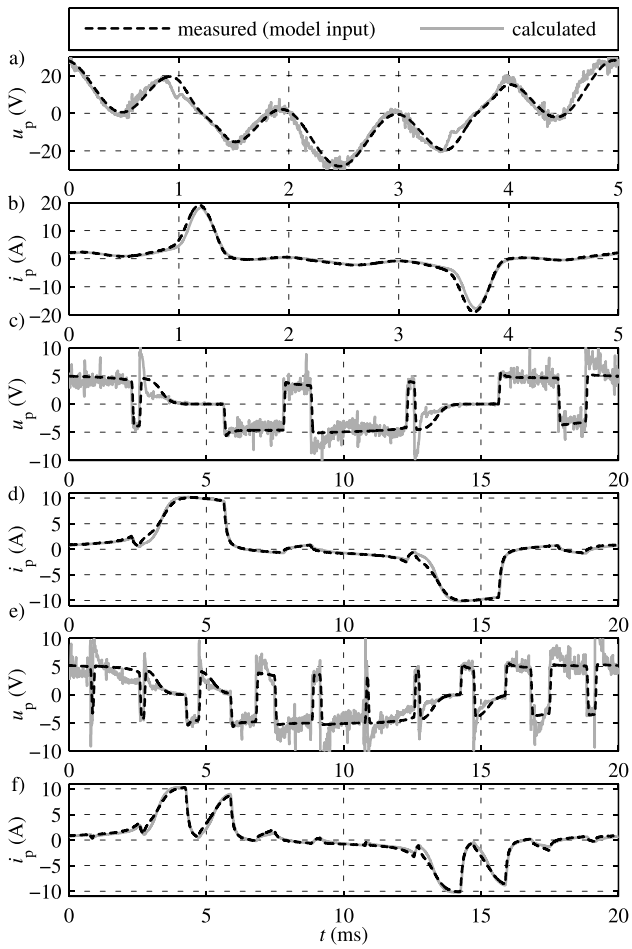

Fig. 1. Measured and calculated excitation voltages u_{p} and currents i_{p} for three different excitation waveforms.

i_{p} are shown in Fig. 1(d) and (f). Note that also for PWM-like excitations, both excitation cases were evaluated. All the variables shown in Fig. 1 are measured and calculated at maximum average densities of magnetic flux of $B_{\max} = 1.5$ T, where the highest deviations between measured and calculated results were observed.

The calculated results show fairly a good agreement with the measurements, where better agreement is achieved when measured voltage u_{p} is used as the model input. When comparing the calculated and measured results, it is evident that for the i_{p} input cases [e.g., input current i_{p} in Fig. 1(b)], the calculated voltages u_{p} [e.g., u_{p} in Fig. 1(a)] contain big ripples, where for the u_{p} input cases the ripple in the corresponding current is not visible. The reason of increased calculated ripple is the direct use of the measured variables, which contain measurement errors. Consequently, the input signal is not smooth, which is influencing the calculated results during the time integration. It is interesting to note that when the measured voltage u_{p} is directly applied to the model as the input, the calculated results become smoother, most probably due to the additional winding equation that serves as a filter of the input signal.

In Fig. 2, the corresponding measured and calculated dynamic hysteresis are shown, where Fig. 2(a) corresponds to Fig. 1(a) and (b), Fig. 2(b) corresponds to Fig. 1(c) and (d), and Fig. 2(c) corresponds to Fig. 1(e) and (f). In Fig. 2(a),

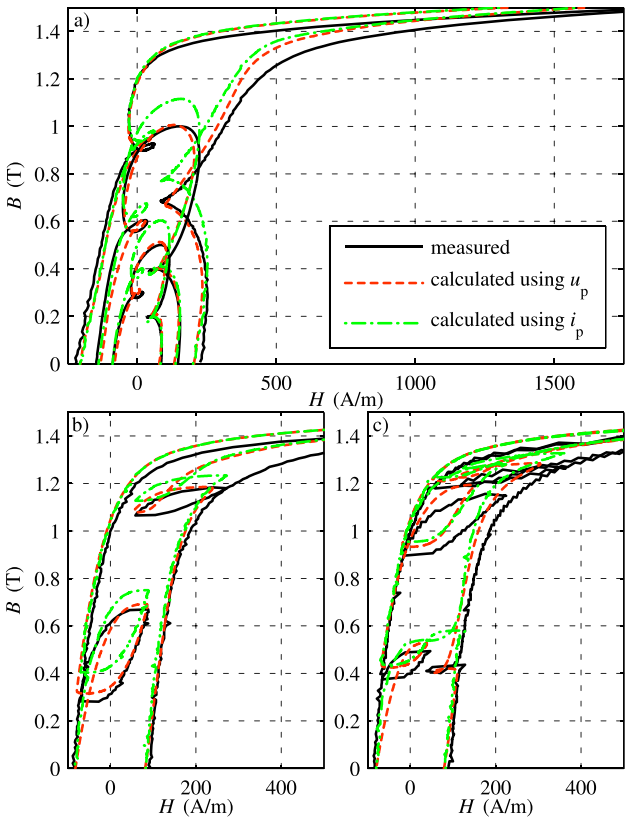

Fig. 2. Measured and calculated dynamic hysteresis loops using voltage and current driven excitations corresponding to excitation waveforms in Fig. 1.

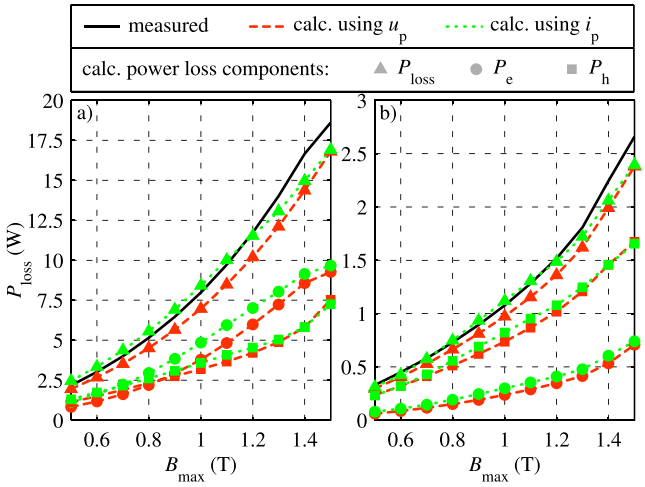

Fig. 3. Comparison between measured and calculated power losses inside the observed SMSS.

also additional dynamic hysteresis loops for $B_{max} = 1$ T and $B_{max} = 0.5$ T are shown.

The obtained results are consistent with the results in Fig. 1, as better agreement is achieved when using the voltage as the model input. Furthermore, from Fig. 2, it is evident that the biggest deviations of the calculated results occur when the magnetic field inside the SMSS approaches saturation. These deviations occur due to the decreased accuracy of the static TLN hysteresis model in discussed area, which is also evident in [8]. For more accurate modeling, a more accurate (preferably history dependent) hysteresis model should be applied.

In Fig. 3, the measured and calculated power loss components inside the observed SMSS are shown, where Fig. 3(a) corresponds to the excitation variables shown in Fig. 1(a) and (b), and Fig. 3(b) corresponds to the excitation variables shown in Fig. 1(c) and (d). The obtained prediction of the power losses shows a good agreement using both discussed excitation cases, where also the decrease of an accuracy is evident when approaching saturation.

IV. Conclusion

This paper provides detailed insight and analysis of two possible utilizations of the discussed MDM for predicting the electromagnetic variables and power loss components under arbitrary excitation waveforms. The discussed MDM was found to be very useful and flexible as it can be used for calculation that is based either on the applied voltage or current in the excitation winding. The model can be therefore easily applied into different circuit simulation software packages. For the presented analysis, the TLN static hysteresis model was applied. The calculated results show that in both input cases, fairly good results are obtained, where the i_p input case is more sensible to the errors in the input signal. The application of the TLN model was found to be questionable when predicting complex magnetizations that include offset minor loops, especially when approaching saturation of the SMSS. The future work will therefore focus on implementation and analysis of more adequate static hysteresis models for a more accurate modeling under arbitrary excitation waveforms.

Acknowledgment

This work was supported by the Slovenian Research Agency (ARRS) under Project P2-0115, Project L2-5489, and Project L2-4114.

References

[1] G. Gruosso and A. Brambilla, "Magnetic core model for circuit simulations including losses and hysteresis," *Int. J. Numer. Model., Electron. Netw., Devices Fields*, vol. 21, no. 5, pp. 309–334, Mar. 2008.

[2] O. Bottauscio, A. Manzin, A. Canova, M. Chiampi, G. Gruosso, and M. Repetto, "Field and circuit approaches for diffusion phenomena in magnetic cores," *IEEE Trans. Magn.*, vol. 40, no. 2, pp. 1322–1325, Mar. 2004.

[3] A. Davoudi, P. L. Chapman, J. Jatskevich, and H. Behjati, "Reduced-order dynamic modeling of multiple-winding power electronic magnetic components," *IEEE Trans. Power Electron.*, vol. 27, no. 5, pp. 2220–2226, May 2012.

[4] J. G. Zhu, S. Y. R. Hui, and V. S. Ramsden, "A generalized dynamic circuit model of magnetic cores for low- and high-frequency applications. I. Theoretical calculation of the equivalent core loss resistance," *IEEE Trans. Power Electron.*, vol. 11, no. 2, pp. 246–250, Mar. 1996.

[5] E. Barbisio, F. Fiorillo, and C. Ragusa, "Predicting loss in magnetic steels under arbitrary induction waveform and with minor hysteresis loops," *IEEE Trans. Magn.*, vol. 40, no. 4, pp. 1810–1819, Jul. 2004.

[6] M. Petrun, V. Podlogar, S. Steentjes, K. Hameyer, and D. Dolinar, "A parametric magneto-dynamic model of soft magnetic steel sheets," *IEEE Trans. Magn.*, vol. 50, no. 4, pp. 1–4, Apr. 2014.

[7] M. Petrun, V. Podlogar, S. Steentjes, K. Hameyer, and D. Dolinar, "Power loss calculation using the parametric magneto-dynamic model of soft magnetic steel sheets," *IEEE Trans. Magn.*, vol. 50, no. 11, Nov. 2014.

[8] J. Tellinen, "A simple scalar model for magnetic hysteresis," *IEEE Trans. Magn.*, vol. 34, no. 4, pp. 2200–2206, Jul. 1998.